International Journal of Food Microbiology 410 (2024) 110486

Contents lists available at ScienceDirect

International Journal of Food Microbiology

journal homepage: www.elsevier.com/locate/ijfoodmicro

Impact of vitamin B_{12} on rhamnose metabolism, stress defense and in-vitro virulence of *Listeria monocytogenes*

Zhe Zeng [a], Lucas M. Wijnands [b], Sjef Boeren [c], Eddy J. Smid [a], Richard A. Notebaart [a], Tjakko Abee [a,*]

[a] Food Microbiology, Wageningen University and Research, Wageningen, the Netherlands
[b] National Institute of Public Health and the Environment, Bilthoven, the Netherlands
[c] Laboratory of Biochemistry, Wageningen University and Research, Wageningen, the Netherlands

ARTICLE INFO

Keywords:
Pathogen
Metabolism
Food
Storage
Food safety
Intestine
Pathogenicity

ABSTRACT

Listeria monocytogenes is a facultative anaerobe which can cause a severe food-borne infection known as listeriosis. *L. monocytogenes* is capable of utilizing various nutrient sources including rhamnose, a naturally occurring deoxy sugar abundant in foods. *L. monocytogenes* can degrade rhamnose into lactate, acetate and 1,2-propanediol. Our previous study showed that addition of vitamin B_{12} stimulated anaerobic growth of *L. monocytogenes* on rhamnose due to the activation of bacterial microcompartments for 1,2-propanediol utilization (*pdu* BMC) with concomitant production of propionate and propanol. Notably, anaerobic 1,2-propanediol metabolism has been linked to virulence of enteric pathogens including *Salmonella* spp. and *L. monocytogenes*. In this study we investigated the impact of B_{12} and BMC activation on i) aerobic and anerobic growth of *L. monocytogenes* on rhamnose and ii) the level of virulence. We observed B_{12}-induced *pdu* BMC activation and growth stimulation only in anaerobically grown cells. Comparative Caco-2 virulence assays showed that these *pdu* BMC-induced cells have significantly higher translocation efficiency compared to non-induced cells (anaerobic growth without B_{12}; aerobic growth with or without B_{12}), while adhesion and invasion capacity is similar for all cells. Comparative proteome analysis showed specific and overlapping responses linked to metabolic shifts, activation of stress defense proteins and virulence factors, with RNA polymerase sigma factor SigL, teichoic acid export ATP-binding protein TagH, DNA repair and protection proteins, RadA and DPS, and glutathione synthase GshAB, previously linked to activation of virulence response in *L. monocytogenes*, uniquely upregulated in anaerobically rhamnose grown *pdu*-induced cells. Our results shed light on possible effects of B_{12} on *L. monocytogenes* competitive fitness and virulence activation when utilizing rhamnose in anaerobic conditions encountered during transmission and the human intestine.

1. Introduction

Listeria monocytogenes is the causative agent of the foodborne illness listeriosis, a rare but severe disease with a high mortality rate in the immunocompromised, very young, and elderly populations. Furthermore, listeriosis also causes abortions in pregnant women (Freitag et al., 2009; Prevention, 2003). Acquisition of this infection is mainly caused by consumption of contaminated food (predominantly ready-to-eat food). *L. monocytogenes* is found ubiquitously in natural environments such as soil, silage, groundwater, sewage and vegetation (Freitag et al., 2009; Radoshevich and Cossart, 2018). The food-borne pathogen can grow at low temperatures and can survive a range of environmental stresses, such as low pH and high salt concentrations (Gandhi and Chikindas, 2007; Radoshevich and Cossart, 2018). Upon ingestion of contaminated food by the host, and following gastric passage, *L. monocytogenes* can bind to epithelial cells in the intestine (Portnoy et al., 2002; Radoshevich and Cossart, 2018). Following entry into epithelial cells mediated by Internalin A (InlA) and Internalin B (InlB), *L. monocytogenes* is internalized into the vacuole (Mengaud et al., 1996; Radoshevich and Cossart, 2018). After the internalization, *L. monocytogenes* applies listeriolysin O (LLO) encoded by *hly* (Portnoy et al., 2002) and two phospholipases, phospholipase A (PlcA) and phospholipase B (PlcB), for vacuolar rupture and escape, which are crucial steps in *L. monocytogenes* pathogenesis (Freitag et al., 2009;

* Corresponding author.
E-mail address: tjakko.abee@wur.nl (T. Abee).

https://doi.org/10.1016/j.ijfoodmicro.2023.110486
Received 3 February 2023; Received in revised form 5 July 2023; Accepted 11 November 2023
Available online 16 November 2023

Radoshevich and Cossart, 2018; Tattoli et al., 2013). Notably, alternative invasion and translocation routes involving LLO and Listeria adhesion protein (LAP) have been described (Burkholder and Bhunia, 2010; Kim and Bhunia, 2013). The molecular mechanisms of how *L. monocytogenes* activates its virulence factors to infect the hosts was summarized in a recent review (Osek and Wieczorek, 2022). All these features make the transmission and contamination of *L. monocytogenes* a severe concern for the food industry (Desai et al., 2019; Gandhi and Chikindas, 2007; Lakicevic et al., 2021; Tasara and Stephan, 2006).

Recent studies on anaerobic growth of *L. monocytogenes* provided evidence that it has the capacity to form proteinaceous organelles so-called bacterial microcompartments (BMCs) which enable extension of its metabolic repertoire by supporting the utilization of rhamnose-derived 1,2-propanediol and ethanolamine derived from degradation of phospholipids (Kerfeld et al., 2018; Zeng et al., 2021a; Zeng et al., 2022; Zeng et al., 2021b; Zeng et al., 2019). BMCs are self-assembling organelles that consist of an enzymatic core that is encapsulated by a semi-permeable protein shell (Kerfeld et al., 2018; Liu, 2021; Yeates et al., 2010). The separation of the encapsulated enzymes from the cytosol is thought to protect the cell from toxic metabolic intermediates such as aldehydes and prevent unwanted side reactions (Kerfeld et al., 2018; Liu, 2021; Yeates et al., 2010). These compartmentalized metabolic pathways may confer a competitive advantage to *L. monocytogenes* over commensal gut microbiota, which typically lack BMC operons and thus are unable to utilize the corresponding substrates in anaerobic conditions (Jakobson and Tullman-Ercek, 2016; Zeng et al., 2021a; Zeng et al., 2022; Zeng et al., 2021b; Zeng et al., 2019). Rhamnose is a deoxyhexose sugar abundant in a range of environments including the human intestine and foods such as oranges, french beans, winter cabbage, and carrots (Vogt et al., 2004). Rhamnose can be degraded in anaerobic conditions into 1,2-propanediol which can be further metabolized by a range of bacteria including *L. monocytogenes* that contain the so-called propanediol utilization (*pdu*) BMCs (Petit et al., 2013; Zeng et al., 2021b). Identification of the rhamnose transport and utilization operon at *lmo2846* to *lmo2851*, including the rhamnose-dependent promoter P(rha), was previously reported (Fieseler et al., 2012). The *L. monocytogenes pdu* cluster forms together with the adjacent ethanolamine utilization (*eut*) cluster and cobalamin synthesis (*cob/cbi*) cluster, a single large locus, referred to as the cobalamin-dependent gene cluster (CDGC) (Anast et al., 2020; Zeng et al., 2019). Previous work suggested that the *pdu* pathway contributes to *L. monocytogenes* establishment in the gastrointestinal tract, while the *eut* pathway may be more important during intracellular replication (Anast et al., 2020; Prentice, 2021). We recently provided evidence that anaerobically ethanolamine and propanediol grown *eut* and *pdu* BMC induced *L. monocytogenes* cells showed significantly higher Caco-2 translocation efficacy in trans-well assays compared to non-induced cells (Zeng et al., 2021c).

We previously reported that addition of vitamin B_{12} enhances anaerobic utilization of rhamnose via *pdu* BMC in *L. monocytogenes* (Zeng et al., 2021b), but the impact of B_{12} on aerobic and anaerobic growth, metabolism and in vitro virulence of *L. monocytogenes* cells grown with rhamnose remains to be determined. We therefore assessed the impact of B_{12} on rhamnose metabolism in aerobically and anaerobically grown *L. monocytogenes*, aligned with metabolic analysis, proteomics and Caco-2 adhesion, invasion and translocation studies.

2. Materials and methods

2.1. Strain and culture conditions

All experiments in this study were carried out with *L. monocytogenes* EGDe aerobically or anaerobically grown at 30 °C in defined medium MWB (Modified Welshimer's broth) (Tsai and Hodgson, 2003). The composition of MWB medium is KH_2PO_4 48.2 mM, Na_2HPO_4 115.5 mM, $MgSO_4$ 1.70 mM, Thiamine 2.96 μM, Riboflavin 1.33 μM, Biotin 2.05 μM, Lipoic acid 24pM, Histidine 0.1 mg/ml, Tryptophan 0.1 mg/ml, Leucine 0.1 mg/ml, Isoleucine 0.1 mg/ml, Valine 0.1 mg/ml, Arginine 0.1 mg/ml, Cysteine 0.1 mg/ml, Methionine 0.1 mg/ml, Glutamine 0.6 mg/ml. Overnight grown cells in Luria Broth (LB) were washed three times in PBS before inoculation into MWB. MWB was supplemented with 20 mM L-rhamnose as sole carbon source with addition of 20 nM B_{12} (defined as *pdu* BMC induced) or without addition of 20 nM B_{12} (defined as *pdu* BMC non-induced). Anaerobic conditions were achieved by Anoxomat Anaerobic Culture System with a gas mixture composed of 10 % CO_2, 5 % H_2, 85 % N_2. OD_{600} measurements in MWB were performed every 12 h for 3 days. Plate counting in MWB to quantity Colony Forming Units (CFUs) was performed every 24 h for 3 days. All the growth measurements were performed with three independent experiments with three technical repeats.

2.2. Analysis of metabolites for Rhamnose metabolism using High Pressure Liquid Chromatography (HPLC)

Samples were taken from the cultures at 0, 24, 48, and 72 h. After centrifugation, the supernatant was collected for the HPLC measurements of rhamnose while the measurement of acetate, lactate, 1,2-propanediol, 1-propanol and propionate was only performed in 72 h. The experiment was performed with three biological replicates. Additionally, the standard curves of all the metabolites were measured in the concentrations 0.1, 1, 5, 10, and 50 mM. HPLC was performed using an Ultimate 3000 HPLC (Dionex) equipped with an RI-101 refractive index detector (Shodex, Kawasaki, Japan), an autosampler and an ion-exclusion Aminex HPX-87H column (7.8 mm × 300 mm) with a guard column (Bio-Rad, Hercules, CA). As the mobile phase 5 mM H_2SO_4 was used at a flow rate of 0.6 ml/min, the column was kept at 40 °C. The total run time was 30 min and the injection volume was 10 μl. All the HPLC measurements were performed with three independent experiments with three technical repeats as described before (Zeng et al., 2021b).

2.3. Proteomics

L. monocytogenes EGDe cultures were aerobically or anaerobically grown at 30 °C in MWB with 20 mM rhamnose adding 20 nM B_{12} or not. Biological duplicates were sampled at 48 h after the inoculation and processed as described before (Zeng et al., 2021b). About 10 mg (wet weight) of cells in 100 μl of 100 mM Tris was sonicated for 30 s twice to lyse the cells. Samples were prepared according to the filter-assisted sample preparation protocol (FASP) with the following steps: reduction with 15 mM dithiothreitol, alkylation with 20 mM acrylamide, and digestion with sequencing-grade trypsin overnight. Each prepared peptide sample was analyzed by injecting (18 μl) into a nano-LC-MS/MS (Thermo nLC1000 connected to a LTQ-Orbitrap XL). Liquid chromatography-mass spectrometry (LC-MS) data with all MS/MS spectra were analyzed with the MaxQuant quantitative proteomics software package. The mass spectrometry proteomics data have been deposited to the ProteomeXchange Consortium via the PRIDE (Vizcaino et al., 2016) partner repository with the dataset identifier PXD025734 for *pdu* BMC induced and *pdu* BMC non-induced conditions.

2.4. Caco-2 adhesion, invasion and translocation

Culturing of Caco-2 cells (human intestinal epithelial cells, ATCC HTB-37) in 12-well plates and production of differentiated cells were carried out as described before (Koomen et al., 2018; Oliveira et al., 2011). *L. monocytogenes* overnight grown cells used for adhesion, invasion and translocation were normalized to get a concentration of 8.4 ± 0.1 log CFU/ml.

For adhesion and invasion experiments, Caco-2 with the inoculum 1.6×10^5 cells/well were seeded into the 12-well tissue culture plates (Corning Inc. ID 3513). Inoculated 12-well plates and were incubated for 12–14 days with the medium refreshing every 2 days at 37 °C to

establish a confluent monolayer of cells. Adhesion and invasion experiments were started by inoculation with 40 µl of late exponential phase cells of Rhamnose *pdu* BMC induced and non-induced *L. monocytogenes* EGDe resulting in an final inoculum of approximately 7.41 log CFU/well. Then the 12 well plates were centrifuged for 1 min at 175 ×*g* to create a proximity between the Caco-2 and *L. monocytogenes* cells.

For adhesion and invasion enumeration, after 1 h anaerobic incubation without gentamicin, *L. monocytogenes* cells that have not adhered to Caco-2 cells were removed by washing three times with PBS buffer. Half of the wells containing Caco-2 cells were lysed with 1 ml of 1 % *v*/v Triton X-100 in PBS and serially diluted in PBS for quantification of the number of adhered and invaded *L. monocytogenes* cells. The other half of the wells of the Caco-2 cells was subsequently incubated anaerobically for 3 h with 0.3 % gentamicin (50 µg/ml, Gibco) to eliminate all extracellular *L. monocytogenes* cells. Thereafter, gentamycin containing medium was removed by washing three times with PBS buffer. The Caco-2 cells were lysed with 1 ml of 1 % v/v Triton X-100 in PBS and serially diluted in PBS for quantification of the number of invaded *L. monocytogenes* EGDe cells.

For translocation experiments, 0.8×10^5 Caco-2 cells per mL were seeded in ThinCert PET inserts (Griener Bio-One 665640) for 12–14 day differentiation. Prior to the translocation assay, wells and inserts were washed three times with PBS, and placed in TCM without gentamycin and fetal bovine serum. Translocation was started by adding 20 µl of late exponential cells of Rhamnose *pdu* BMC induced and non-induced *L. monocytogenes* EGDe cells into the inserts, resulting in an inoculum of approximately 7.17 log CFU/well. After centrifuging the Transwell plates for 1 min at 175 ×g, the plates were incubated 2 h anaerobically. After incubation, the inserts were removed with a sterile forceps and discarded. The contents in the wells was collected for quantification of the translocated number of *L. monocytogenes* EGDe cells.

2.5. Venn diagram analysis and STRING networks analysis

The protein IDs of significantly changed proteins from Supplementary Tables 1, 2 and 3 were uploaded to the BioVenn online server (Hulsen et al., 2008) taking the default setting to generate Venn diagrams. The analysis of Venn diagrams and details of overlaps in upregulated proteins are shown in Supplementary Table 4. Overlapping proteins from the Venn diagram were transferred to the STRING online server (Szklarczyk et al., 2019) for multiple proteins analysis of functional interaction using sources such as co-expression, genomic neighbourhood and gene fusion.

Statistical analyses were performed in Prism 8.0.1 for Windows (GraphPad Software). As indicated in the figure legend, Statistical significances are shown in ***, $P < 0.001$; *, $P < 0.05$; ns, $P > 0.05$ with Holm-Sidak *t*-test.

3. Results

3.1. Impact of vitamin B_{12} on L. monocytogenes grown on rhamnose

We first examined the impact of B_{12} on aerobic and anaerobic growth of *L. monocytogenes* EGDe in MWB defined medium without and with added vitamin B_{12} (Fig. 1). In Fig. 1A, *L. monocytogenes* showed a similar aerobic growth in MWB defined medium plus 20 mM rhamnose with or without 20 mM B_{12}, where OD_{600} reaches a maximum of approximately 0.56 after 72 h. But for anaerobic conditions, in MWB defined medium supplied with 20 mM rhamnose, OD_{600} reaches a maximum of about 0.37 after 48 h, while in MWB supplied with 20 mM rhamnose and 20 nM B_{12}, OD_{600} continues to increase after 48 h reaching a significant higher OD_{600} of 0.51 at 72 h as described before (Zeng et al., 2021b). The growth phenotypes indicate that addition of 20 nM B_{12} into MWB defined medium plus 20 mM rhamnose stimulates anaerobic growth of *L. monocytogenes*, but has no significant effect on aerobic growth with rhamnose which is already enhanced compared to that in anaerobic conditions. Next, utilization of rhamnose in aerobic and anaerobic conditions with or without B_{12} was quantified. The aerobic growth of *L. monocytogenes* with or without B_{12} appears similar including the rhamnose degradation capacity, that showed complete consumption of 20 mM rhamnose within 72 h (Fig. 1B). Complete consumption of rhamnose was also observed in anaerobically grown cells in MWB plus 20 mM rhamnose and B_{12}, whereas 3.5 mM of rhamnose was still present at 72 h in MWB plus 20 mM rhamnose without added B_{12}. These results indicate that addition of B_{12} stimulates anaerobic growth and rhamnose metabolism of *L. monocytogenes* EGDe, while no significant impact of B_{12} was detected with aerobically grown cells.

3.2. Impact of B_{12} on aerobic or anaerobic metabolism of rhamnose

Metabolite production in the different growth conditions was analyzed by HPLC. As shown in Fig. 2, at 72 h, rhamnose was degraded by *L. monocytogenes* EGDe into acetate, lactate and 1,2-propanediol in anaerobic and aerobic conditions with or without B_{12}, albeit to different

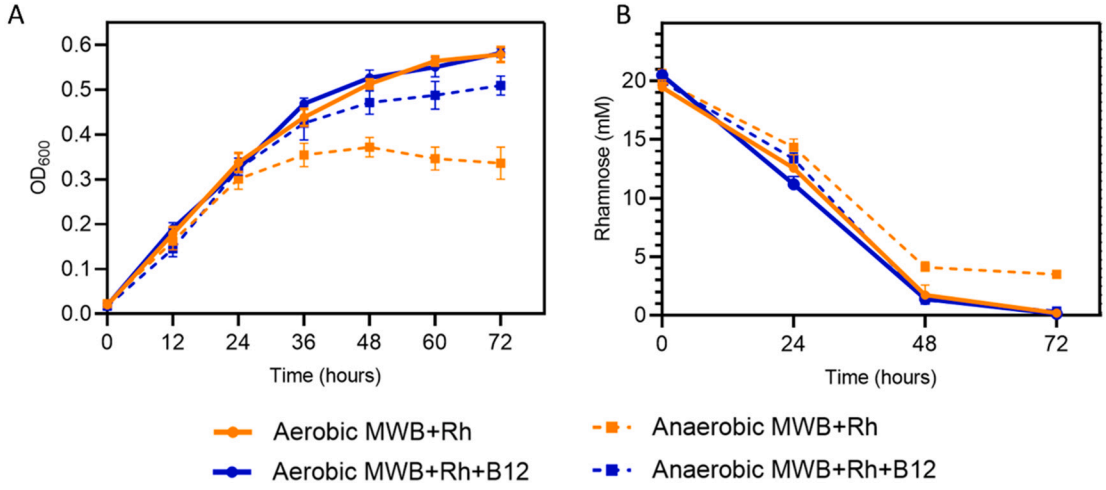

Fig. 1. Growth and Rhamnose catabolism of *L. monocytogenes* EGDe in MWB medium with 20 mM Rhamnose.
(A) Impact of vitamin B_{12} on aerobic and anaerobic growth of *L. monocytogenes* EGDe in MWB medium with 20 mM Rhamnose; (1B) Rhamnose utilization. Orange lines with closed circles represent *L. monocytogenes* grown in MWB medium with 20 mM Rhamnose, while blue lines with closed circles represent *L. monocytogenes* grown in MWB medium with 20 mM Rhamnose and 20 nM B_{12}. Solid lines represent aerobic conditions, and striped lines represent anaerobic conditions; data of anaerobic conditions published in (Zeng et al., 2021b). Results from three independent experiments are expressed and visualized as means and standard errors.

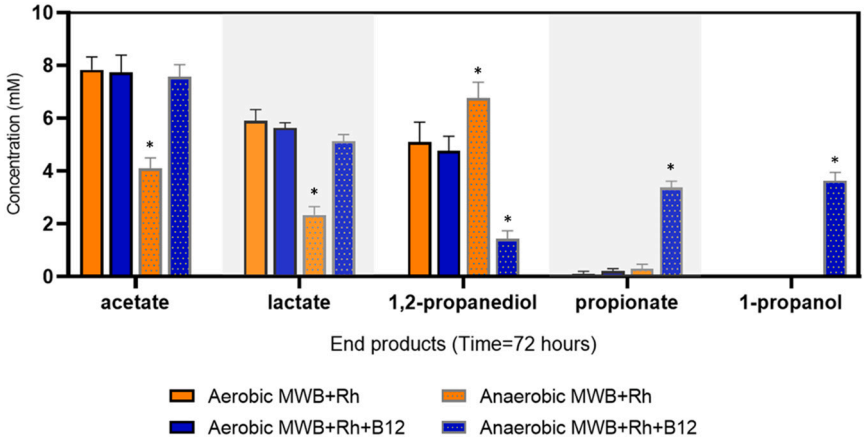

Fig. 2. Metabolites from rhamnose metabolism of *L. monocytogenes* EGDe aerobically or anaerobically grown in MWB with 20 mM Rhamnose with/without 20 nM vitamin B_{12}.
Orange bars represent *L. monocytogenes* grown in MWB medium with 20 mM Rhamnose, while blue bars represent *L. monocytogenes* grown in MWB medium with 20 mM Rhamnose and 20 nM B_{12}. Metabolites are grouped as indicated in X-axis, successively, acetate, lactate, 1,2-propanediol, propionate and 1-propanol. Bars with black outline represent aerobic condition, and Bars with gray outline and filled pattern represent anaerobic condition; data of anaerobic condition published in (Zeng et al., 2021b). Results from three independent experiments are expressed and visualized as means and standard errors.

levels. Metabolites following growth in MWB medium plus 20 mM rhamnose with and without B_{12} in aerobic conditions, showed no significant differences in acetate, lactate and 1,2-propanediol production, in line with the corresponding similar growth phenotypes and rhamnose utilization in Fig. 1. Notably, the type and amount of end products formed during rhamnose utilization in anaerobic conditions with B_{12} added, are significantly different from all other tested conditions, and include 4.1 mM acetate, 2.3 mM lactate, 1.4 mM 1,2-propanediol, and 3.2 mM propionate and 3.6 mM 1-propanol, indicative of activated *pdu* BMC. These data provide evidence for specific activation of *pdu* BMC in *L. monocytogenes* during growth on rhamnose in anaerobic conditions with B_{12} added to the medium.

3.3. Proteome analysis of aerobically and anaerobically grown *L. monocytogenes* on rhamnose without and with added B_{12}

Comparative proteomics analysis identified differentially expressed proteins in cells grown in MWB medium plus 20 mM rhamnose with or without B_{12} in aerobic and anaerobic conditions (Fig. 3). Fig. 3A shows data for MWB plus 20 mM rhamnose in anaerobic condition compared to MWB plus 20 mM rhamnose in aerobic condition. Obviously, 21 proteins out of 23 Pdu proteins (yellow dots encircled in black lines in Fig. 3A) in the BMC-dependent 1,2-propanediol utilization cluster, are upregulated in anaerobically grown cells on rhamnose compared to aerobically grown cells (details in Supplementary Table 1). Notably, despite expression of Pdu proteins, no production of *pdu* BMC signature metabolites propionate and 1-propanol was detected as shown above (Fig. 2), in line with our previously reported data (Zeng et al., 2021b), that showed only presence of BMCs and activation of *pdu* BMC in anaerobically rhamnose grown cells with added B_{12}. Our data extend previous RNAseq studies that showed slight increase in *pdu* expression in the presence of propanediol, and highest expression when B_{12} was also present (Mellin et al., 2013; Salazar et al., 2013). The lack of *pdu* BMC activation in anaerobic MWB plus rhamnose conditions, suggests that the observed activation of B_{12} synthesis enzymes does not result in the production of sufficiently high levels of (de novo) B_{12} to trigger full induction (Fig. 3A and Supplementary Table 5). Comparative analysis of anaerobically versus aerobically grown cells, points to repression of propanediol-induced *pdu* expression in the latter condition. Notably, highlighted virulence factors in the volcano plot (Fig. 3A), show that actin assembly-inducing protein ActA, Listeriolysin O (LLO) encoded by *hly*, Listeriolysin regulatory protein PrfA, and phospholipase C encoded by *clpB*, are slightly upregulated in anaerobic growth compared to aerobic growth of *L. monocytogenes* on rhamnose, while PlcA, phospholipase A, shows no significant difference, and internalin C was repressed. Rha proteins for rhamnose utilization including rhaA, rhaB, rhaD, rhaM and lmo2850 contained in the *rha* cluster, are all slightly upregulated in anaerobic growth compared to aerobic growth of *L. monocytogenes* on rhamnose. Anaerobic growth of *L. monocytogenes* on rhamnose with added B_{12} results in increased expression of Pdu proteins (Fig. 3C) and presence of BMCs was evidenced by TEM (shown in our recent study (Zeng et al., 2021b)). Rha proteins do not show significant differences, while PrfA, PlcB and ActA are induced, but PlcA, hly and InlC are repressed in MWB plus 20 mM rhamnose with B_{12} compared cells grown without B_{12} (Details in Supplementary Table 3). Notably, addition of B_{12} and induction of *pdu* BMC in anaerobic conditions, results in a significant repression of B_{12} biosynthesis proteins (8 identified B_{12} proteins, Fig. 3C). Reduced expression is also seen in aerobically grown cells, where only 4 B_{12} biosynthesis proteins are identified (Fig. 3B). Combining these results suggests that addition of B_{12} has a repressive effect on B_{12} biosynthesis proteins in anaerobically rhamnose grown *L. monocytogenes* EGDe cells, with the B_{12} biosynthesis proteins largely repressed in aerobically grown cells (Details in Supplementary Table 5).

3.4. Stress and virulence proteins triggered by B_{12}-activated *pdu* BMC

The Venn diagram provides an overview of differentially expressed proteins in conditions without and with added B_{12} in aerobically and anaerobically rhamnose grown *L. monocytogenes* (Fig. 4). As shown in Fig. 4A, 145 proteins (Group A, red pie chart) are upregulated more than two fold in anaerobic MWB plus rhamnose with B_{12} compared to anaerobic condition without B_{12}, and 81 proteins (Group B, yellow pie chart) are upregulated more than two fold in aerobic condition with B_{12} compared to aerobic condition without B_{12}, while 162 proteins (Group C, blue pie chart) are upregulated more than two fold in anaerobic condition without B_{12} compared to aerobic condition without B_{12} (details in Supplementary Table 4). The overlap of group A and group B contains 25 proteins that are upregulated in anaerobic and aerobic rhamnose conditions with added B_{12}, with eight of the proteins present also in group C. The proportion in red group A without overlap with other groups represents 103 proteins upregulated in *pdu* BMC induced cells anaerobically grown in rhamnose with added B_{12} (Fig. 4B, details in Supplementary Table 4). STRING protein-protein interaction analysis of these 103 proteins uniquely upregulated in anaerobically rhamnose

grown *pdu* BMC induced *L. monocytogenes* cells, points to differential expression of a range of ribosomal and ribosome-associated proteins, including RplB, 50S ribosomal protein L28, RpsO, 30S ribosomal protein S15, Rnc, ribonuclease 3, involved in the processing of primary rRNA, and YbeY, an endoribonuclease involved in late-stage 70S ribosome maturation, while other proteins point to metabolic shifts, activation of stress defense, and links to virulence, such as RNA polymerase sigma factor SigL, Teichoic acids export ATP-binding protein, TagH, DNA repair and protection proteins RadA and DPS, and glutathione synthase GshAB, previously linked to activation of virulence response in *L. monocytogenes* (Liu et al., 2017; Raimann et al., 2009; Reniere et al., 2016). In addition, *pdu* BMC induced cells share a range of other virulence factors also expressed in anaerobic non-induced cells (Supplementary Table 3), including endopeptidase p60 (Iap), (higher expressed in *pdu* BMC cells), Listeriolysin regulatory protein (PrfA), 1-phosphatidylinositol phosphodiesterase (PlcA), Phospholipase C (PlcB), Actin assembly-inducing protein (ActFA), Internalin C (InlC) and Internalin B (InlB) (both higher expressed in in non-induced cells), and bi-functional Listeria associated protein (LAP, lmo1634) (Freitag et al., 2009; Kim and Bhunia, 2013; Lungu et al., 2009; Radoshevich and Cossart, 2018; Scortti et al., 2007). Next, in vitro virulence assays were performed to compare performance of anaerobic *pdu* BMC induced cells to non-induced anaerobic and aerobic cells.

3.5. Impact of B_{12} on Caco-2 cell adhesion, invasion and translocation of *L. monocytogenes* grown aerobically or anaerobically on rhamnose

To address the impact of B_{12} on *L. monocytogenes* in vitro virulence, we conducted adhesion, invasion and translocation assays with Caco-2 cells using rhamnose *pdu* BMC induced and non-induced cells grown anaerobically and aerobically. As shown in Fig. 5, *L. monocytogenes* cells grown anaerobically or aerobically in MWB plus 20 mM rhamnose with or without B_{12} show similar adhesion and invasion efficacy of ~5.2 log and ~4.1 log CFU/well, respectively. Strikingly, the ability to translocate Caco-2 cells monolayers in a trans-well system, is significantly higher for *L. monocytogenes* cells grown anaerobically in MWB plus rhamnose with B_{12} compared to the other cells (~1 log CFU/well improvement), grown anaerobically without B_{12} and aerobically without and with B_{12} (Fig. 5). These results indicate similar adhesion and invasion capacity of all four tested cell types, while anaerobically rhamnose grown *pdu* BMC induced *L. monocytogenes* cells show significantly higher translocation efficacy compared to the three non-induced cell types.

4. Discussion

The results in this study show a unique stimulating effect of B_{12} supplementation on anaerobic growth of *L. monocytogenes* with rhamnose, linked to *pdu* BMC activation and production of signature metabolites propionate and propanol, while no effect on rhamnose metabolism is observed in aerobic conditions. Growth in the latter condition with and without added B_{12} results in higher biomass production compared to anaerobically grown cells with and without added B_{12}, conceivably due to increased energy generation via respiration (Lungu et al., 2009). Observed growth stimulation in rhamnose *pdu* BMC induced cells compared to non-induced cells is in line with previously described results (Zeng et al., 2021b).

L. monocytogenes has to cope with anaerobic conditions encountered during transmission along the food chain, for example in modified atmosphere and vacuum-packed foods, and in the GI tract. Upregulation of the *pdu* operon related to rhamnose metabolism has been found in *L. monocytogenes* grown on vacuum-packed cold smoked salmon and in co-cultures with cheese rind bacteria (Anast and Schmitz-Esser, 2020; Kaszoni-Rückerl et al., 2020; Tang et al., 2015). Notably, a significant upregulation of Pdu proteins involved in 1,2-propanediol utilization is observed in anaerobic MWB plus 20 mM rhamnose grown cells compared to aerobic MWB plus 20 mM rhamnose grown cells. This could point to activation of 1,2-propanediol utilization, in line with concomitant increase in expression of B_{12} synthesis enzymes in these anaerobically rhamnose grown *L. monocytogenes* cells, but HPLC analysis

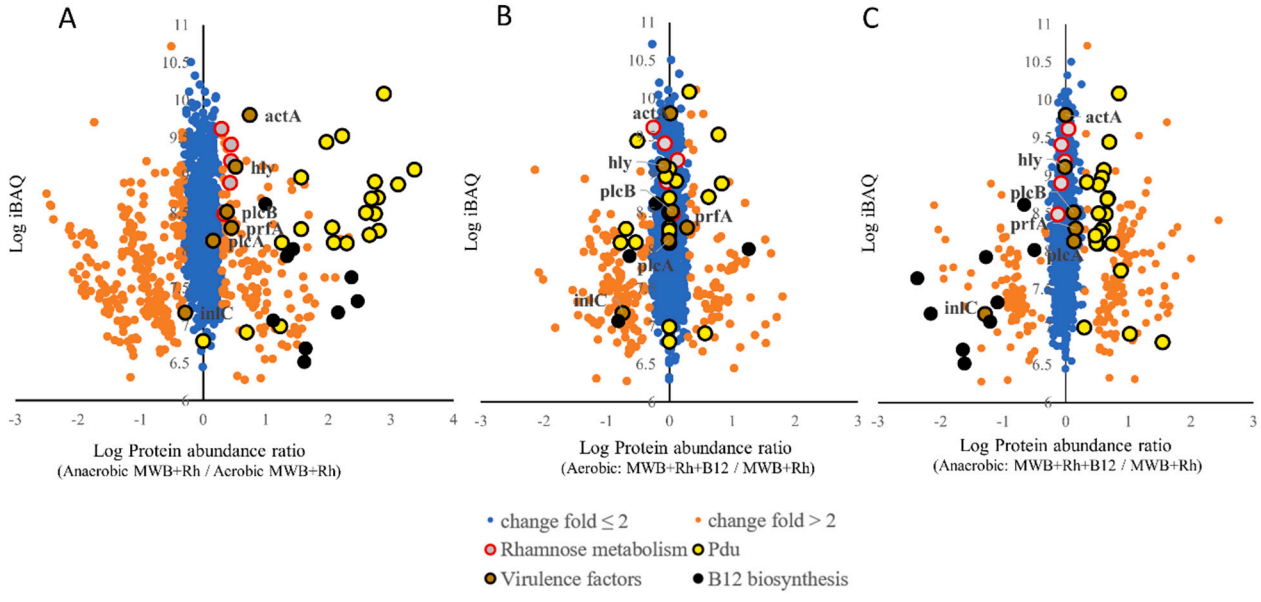

Fig. 3. Proteomic analysis of *L. monocytogenes* EGDe aerobically or anaerobically grown in MWB with 20 mM Rhamnose with/without 20 nM vitamin B_{12}. (A) Proteomic ratio plot of *L. monocytogenes* anaerobically grown in MWB plus 20 mM rhamnose compared to *L. monocytogenes* aerobically grown in MWB plus 20 mM rhamnose, (full list in Supplementary Table 1). (B) Proteomic ratio plot of *L. monocytogenes* aerobically grown in MWB plus 20 mM rhamnose and 20 nM B_{12} compared to *L. monocytogenes* aerobically grown in MWB plus 20 mM rhamnose, (full list in Supplementary Table 2). (C) Proteomic ratio plot of *L. monocytogenes* anaerobically grown in MWB plus 20 mM rhamnose and 20 nM B12 compared to *L. monocytogenes* anaerobically grown in MWB plus 20 mM rhamnose, (full list in Supplementary Table 3). Fold change ≤ 2 in blue, fold change > 2 in light orange, proteins in the *pdu* cluster are black encircled in yellow, and proteins in the rhamnose cluster are red encircled in gray. Virulence factors in Supplementary Table 4 are black encircled in dark orange. Proteins encoded by the *cob/cbi* operon for B12 biosynthesis are shown in black.

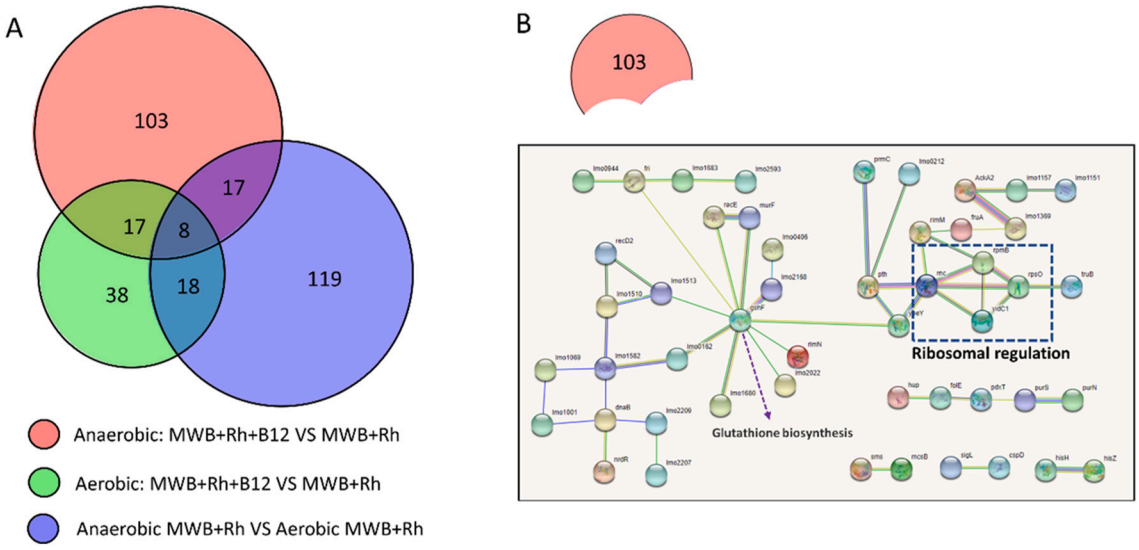

Fig. 4. Proteomics analysis of vitamin B_{12} impact on *L. monocytogenes* EGDe general stress response and virulence factors.
(A) Venn diagram of overlapping upregulated proteins among three groups. Group A in red: anaerobic growth of *L. monocytogenes* on MWB with 20 mM rhamnose and 20 nM B_{12}, compared to MWB with 20 mM rhamnose without B_{12}; Group B in yellow: aerobic growth of *L. monocytogenes* on MWB with 20 mM rhamnose and 20 nM B_{12} compared MWB with 20 mM rhamnose without B_{12}; Group C in blue: anaerobic growth of *L. monocytogenes* on MWB with 20 mM rhamnose without B_{12} compared aerobic MWB with 20 mM rhamnose without B_{12}; (B) STRING analysis of proteins specifically upregulated by the addition of B_{12} in anaerobically grown *L. monocytogenes* in MWB with 20 mM rhamnose; Nodes represent proteins, and lines represent interactions, disconnected proteins are not shown in the network (details in Supplementary Table 4).

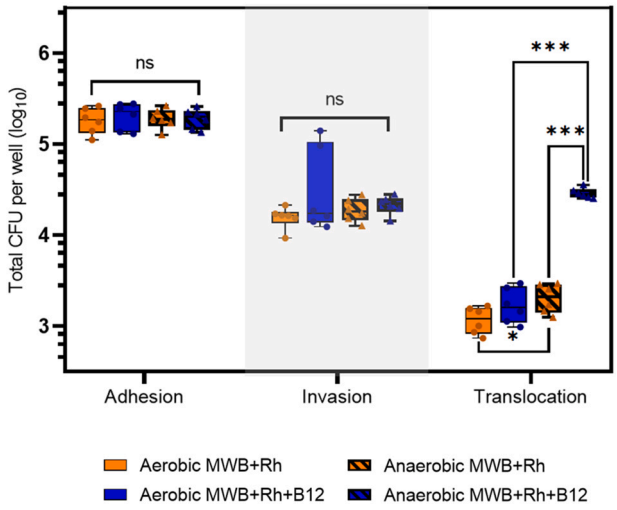

Fig. 5. Caco-2 cell assays with *L. monocytogenes* EGDe aerobically or anaerobically grown in MWB with 20 mM Rhamnose with/without 20 nM vitamin B_{12}. Orange bars represent *L. monocytogenes* grown in MWB medium with 20 mM Rhamnose, while blue bars represent *L. monocytogenes* grown in MWB medium with 20 mM Rhamnose and 20 nM B_{12}. Bars without filled pattern represent aerobic conditions, and Bars with filled pattern represent anaerobic conditions. X axis shows three groups of columns with results from adhesion, invasion and translocation assays. Y axis is the total CFU per well in log10 after the assays while initial inputs for adhesion and invasion are 7.41 ± 0.02 in log10 CFU per well and the initial inputs for translocation are 7.17 ± 0.03 in log10 CFU per well. Statistical significance is indicated (*** means $P \leq 0.001$; * means $P \leq 0.05$; ns means >0.05 by Holm-Sidak *t*-test).

indicates that *pdu* BMC signature metabolites, propionate and 1-propanol are not produced, in line with absence of BMCs in TEM analysis (Zeng et al., 2021b). Addition of B_{12} to anaerobically rhamnose grown cells results in further, significantly increased, expression of Pdu proteins, and activation of *pdu* BMC as evidenced by the production of propionate and 1-propanol (Fig. 2), and presence of BMCs detected by TEM (Zeng et al., 2019, 2021b). It is conceivable, that B_{12} dependent activation of *pdu* BMC in anaerobic conditions is not only crucial due to the role of B_{12} as a cofactor for the signature enzyme PduCDE, a B_{12}-dependent diol dehydratase (Zeng et al., 2019), but also because the PduCDE-B_{12} complex plays a role in triggering the construction of BMC with the shell proteins thereby encasing *pdu* enzymes, with the respective signature peptide sequences directing enzyme complexes to the correct locations inside the microcompartment (Kennedy et al., 2021; Kerfeld et al., 2018; Liu et al., 2021; Stewart et al., 2021). Our results with aerobically and anaerobically rhamnose grown cells in MWB medium, indicate that RNAseq data of *pdu* operon, including identification of factors involved in control of gene expression, such as regulator PocR, B_{12}-dependent riboswitch(es) and sRNAs (Lebreton and Cossart, 2017; Mellin et al., 2013), require confirmation by proteomics, TEM and metabolic profiling to enable conclusions about activation of functional *pdu* BMC in *L. monocytogenes*.

B_{12}-dependent activation of *pdu* BMC in *L. monocytogenes* also results in additional cellular responses. Comparative proteome analysis identified 103 proteins uniquely upregulated in *pdu* BMC induced cells with functions in protein synthesis, ribosomal proteins and ribosome-associated proteins, and in metabolism and stress defense, including RNA polymerase sigma factor SigL, Teichoic acids export ATP-binding protein, TagH, DNA repair and protection proteins RadA and DPS, and glutathione (GSH) synthase GshF, a multidomain protein encoded by *gshAB* (Figs. 3 and 4, Supplementary Tables 2 and 3). GshF mediated production of glutathione was recently linked to activation of virulence response in *L. monocytogenes*, with glutathione acting as an allosteric activator of Listeriolysin regulatory protein PrfA (Reniere et al., 2016). Notably, a range of virulence factors is expressed both in anaerobic *pdu* BMC induced and non-induced cells (Supplementary Table 3), including regulatory protein PrfA, phosphatidylinositol phosphodiesterase (PlcA), Phospholipase C (PlcB), listeriolysin O (LLO), Actin assembly-inducing protein (ActA), Internalin C (InlC) and Internalin B (InlB), and bifunctional Listeria associated protein (LAP, lmo1634) (Burkholder and Bhunia, 2010; Kim and Bhunia, 2013). Extracellular cell wall associated LAP, has been suggested to play a role in *L. monocytogenes* interaction with the host by affecting cellular redistribution of epithelial junction

proteins enhancing bacterial translocation (Burkholder and Bhunia, 2010; Kim and Bhunia, 2013). Analysis of proteomes from aerobically rhamnose grown cells without and with added B_{12} (Supplementary Tables 1 and 3), also indicate (low level) presence of the virulence factors described above.

Our comparative in vitro virulence assays indicate similar Caco-2 adhesion and invasion capacity of aerobically and anaerobically rhamnose grown cells without and with added B_{12}, while only anaerobically rhamnose grown *pdu* BMC induced *L. monocytogenes* cells show significantly higher Caco-2 translocation efficacy compared to the three other non-induced cell types. These results suggest that anaerobically rhamnose grown *pdu* BMC primed *L. monocytogenes* cells show enhanced transcellular and/or paracellular translocation in the Caco-2 cells trans-well assay. Transcellular translocation involves *L. monocytogenes* binding and internalization into epithelial cells, and proceeds by intracellular replication and/or movement into neighboring epithelial cells by hijacking host cellular machinery via PrfA-activated virulence factors (de las Heras et al., 2011; Nadon et al., 2002; Scortti et al., 2007). Based on similar performance in our *L. monocytogenes* EGDe adhesion and invasion studies, with 1 h and 3 h incubation periods, respectively, it is unlikely that enhanced translocation capacity, with a 2 h incubation period, is linked to enhanced transcellular performance of rhamnose *pdu* BMC primed cells. An alternative explanation could be offered by enhanced paracellular translocation of *L. monocytogenes* cells, i.e., passing through an intercellular space between the Caco-2 cells, such as tight junctions (Drolia et al., 2018; Pentecost et al., 2006). Tight junctions play a major role in maintaining the integrity and selective permeability of the intestinal barrier (Chelakkot et al., 2018; Drolia et al., 2018; Pentecost et al., 2006). Different strategies are used by pathogens aimed at destabilizing tight junctions, and roles for internalin A, LAP and listeriolysin O (LLO) in paracellular translocation of *L. monocytogenes* have been reported (Chelakkot et al., 2018; Drolia et al., 2018; Kim and Bhunia, 2013). Combined with adapted physiology and metabolic shifts in *pdu* BMC induced cells including activated stress defense and GSH production, action of LAP and/or LLO, may have supported enhanced translocation in the trans-well assay. Notably, our previous results with anaerobically grown *L. monocytogenes* EGDe in LB medium with propanediol or ethanolamine, with and without added B_{12}, showed similar adhesion and invasion capacity, but significantly higher translocation efficacy of respective *pdu* BMC and *eut* BMC induced cells (Zeng et al., 2021c).

We previously provided evidence for *L. monocytogenes* growth stimulation via B_{12} dependent activation of *pdu* BMC in anaerobically propanediol and rhamnose grown cells (Zeng et al., 2021b; Zeng et al., 2019). Combined with the suggested role in foods and processing environments (Anast and Schmitz-Esser, 2020; Kaszoni-Rückerl et al., 2020; Tang et al., 2015), *pdu* BMC may contribute to competitive fitness of *L. monocytogenes* during transmission in the food chain. Additionally, *pdu* BMC may enhance fitness in the intestine, based on previous observations that showed reduced *L. monocytogenes* persistence in stool and ileal colonization of female BALB/c mice of a *pdu*D (subunit of propanediol dehydratase) deletion mutant compared to the wild type (Schardt et al., 2017). Our results obtained in Caco-2 virulence assays may point to an additional impact of (rhamnose) *pdu* BMC activation on *L. monocytogenes* interaction with host intestinal epithelial barrier, more specifically, translocation of cells via tight junctions. In this study we used *L. monocytogenes* EGDe and Caco-2 trans-well assays as an in vitro virulence model. Although this approach allows a well-defined comparative analysis of B12 dependent Rhamnose Pdu BMC-induced *L. monocytogenes* EGDe cells versus non-induced cells, these conditions are different from in vivo conditions, as the influence of diet on host immune function and the gastrointestinal microbiota are not taken into account (Las Heras et al., 2022). In addition, the overview of a range of newly available mouse models and the link with relevant parameters of human infection (Herzog et al., 2023), offers opportunities to select optimal mouse models for future studies to address relevant in vivo aspects in the virulence of rhamnose derived Pdu BMC-induced *L. monocytogenes* using isolates from different clinical clonal complexes (Moura et al., 2021). Based on recent insights that BMCs are found in an approximate 20–25 % of (human) microbiota (Ravcheev et al., 2019; Sutter et al., 2021), the combination of in silico, in vitro and in vivo studies is required to advance our understanding of the role of BMCs in human intestinal health and disease.

Supplementary data to this article can be found online at https://doi.org/10.1016/j.ijfoodmicro.2023.110486.

Declaration of competing interest

The authors have no affiliation with any organization with a direct or indirect financial interest in the subject matter discussed in the manuscript.

Data availability

Data will be made available on request.

Acknowledgements

Z.Z. was supported by a grant from the China Scholarship Council.

References

Anast, J.M., Schmitz-Esser, S., 2020. The transcriptome of *Listeria monocytogenes* during co-cultivation with cheese rind bacteria suggests adaptation by induction of ethanolamine and 1,2-propanediol catabolism pathway genes. PLoS One 15, e0233945.

Anast, J.M., Bobik, T.A., Schmitz-Esser, S., 2020. The Cobalamin-dependent gene cluster of *Listeria monocytogenes*: implications for virulence, stress response, and food safety. Front. Microbiol. 11.

Burkholder, K.M., Bhunia, A.K., 2010. *Listeria monocytogenes* uses Listeria adhesion protein (LAP) to promote bacterial transepithelial translocation and induces expression of LAP receptor Hsp60. Infect. Immun. 78, 5062–5073.

Chelakkot, C., Ghim, J., Ryu, S.H., 2018. Mechanisms regulating intestinal barrier integrity and its pathological implications. Exp. Mol. Med. 50, 1–9.

de las Heras, A., Cain, R.J., Bielecka, M.K., Vazquez-Boland, J.A., 2011. Regulation of Listeria virulence: PrfA master and commander. Curr. Opin. Microbiol. 14, 118–127.

Desai, A.N., Anyoha, A., Madoff, L.C., Lassmann, B., 2019. Changing epidemiology of *Listeria monocytogenes* outbreaks, sporadic cases, and recalls globally: a review of ProMED reports from 1996 to 2018. Int. J. Infect. Dis. 84, 48–53.

Drolia, R., Tenguria, S., Durkes, A.C., Turner, J.R., Bhunia, A.K., 2018. Listeria adhesion protein induces intestinal epithelial barrier dysfunction for bacterial translocation. Cell Host Microbe 23 (470–484), e477.

Fieseler, L., Schmitter, S., Teiserskas, J., Loessner, M.J., 2012. Rhamnose-inducible gene expression in *Listeria monocytogenes*. PLoS One 7, e43444.

Freitag, N.E., Port, G.C., Miner, M.D., 2009. *Listeria monocytogenes*—from saprophyte to intracellular pathogen. Nat. Rev. Microbiol. 7, 623–628.

Gandhi, M., Chikindas, M.L., 2007. Listeria: a foodborne pathogen that knows how to survive. Int. J. Food Microbiol. 113, 1–15.

Herzog, M.K., Cazzaniga, M., Peters, A., Shayya, N., Beldi, L., Hapfelmeier, S., Heimesaat, M.M., Bereswill, S., Frankel, G., Gahan, C.G.M., Hardt, W.D., 2023. Mouse models for bacterial enteropathogen infections: insights into the role of colonization resistance. Gut Microbes 15, 2172667.

Hulsen, T., de Vlieg, J., Alkema, W., 2008. BioVenn - a web application for the comparison and visualization of biological lists using area-proportional Venn diagrams. BMC Genomics 9, 488.

Jakobson, C.M., Tullman-Ercek, D., 2016. Dumpster diving in the gut: bacterial microcompartments as part of a host-associated lifestyle. PLoS Pathog. 12, e1005558.

Kaszoni-Rückerl, I., Mustedanagic, A., Muri-Klinger, S., Brugger, K., Wagner, K.H., Wagner, M., Stessl, B., 2020. Predominance of distinct *Listeria innocua* and *Listeria monocytogenes* in recurrent contamination events at dairy processing facilities. Microorganisms 8.

Kennedy, N.W., Mills, C.E., Nichols, T.M., Abrahamson, C.H., Tullman-Ercek, D., 2021. Bacterial microcompartments: tiny organelles with big potential. Curr. Opin. Microbiol. 63, 36–42.

Kerfeld, C.A., Aussignargues, C., Zarzycki, J., Cai, F., Sutter, M., 2018. Bacterial microcompartments. Nat. Rev. Microbiol. 16 (5), 277–290.

Kim, H., Bhunia, A.K., 2013. Secreted Listeria adhesion protein (Lap) influences Lap-mediated *Listeria monocytogenes* paracellular translocation through epithelial barrier. Gut Pathog. 5, 1–11.

Koomen, J., den Besten, H.M., Metselaar, K.I., Tempelaars, M.H., Wijnands, L.M., Zwietering, M.H., Abee, T., 2018. Gene profiling-based phenotyping for identification of cellular parameters that contribute to fitness, stress-tolerance and virulence of *Listeria monocytogenes* variants. Int. J. Food Microbiol. 283, 14–21.

Lakicevic, B.Z., Den Besten, H.M.W., De Biase, D., 2021. Landscape of stress response and virulence genes among *Listeria monocytogenes* strains. Front. Microbiol. 12, 738470.
Las Heras, V., Melgar, S., MacSharry, J., Gahan, C.G.M., 2022. The influence of the western diet on microbiota and gastrointestinal immunity. Annu. Rev. Food Sci. Technol. 13, 489–512.
Lebreton, A., Cossart, P., 2017. RNA-and protein-mediated control of *Listeria monocytogenes* virulence gene expression. RNA Biol. 14, 460–470.
Liu, L.N., 2021. Bacterial metabolosomes: new insights into their structure and bioengineering. Microb. Biotechnol. 14, 88–93.
Liu, Y., Orsi, R.H., Boor, K.J., Wiedmann, M., Guariglia-Oropeza, V., 2017. Home alone: elimination of all but one alternative sigma factor in *Listeria monocytogenes* allows prediction of new roles for σB. Front. Microbiol. 8, 1910.
Liu, L.-N., Yang, M., Sun, Y., Yang, J., 2021. Protein stoichiometry, structural plasticity and regulation of bacterial microcompartments. Curr. Opin. Microbiol. 63, 133–141.
Lungu, B., Ricke, S., Johnson, M., 2009. Growth, survival, proliferation and pathogenesis of *Listeria monocytogenes* under low oxygen or anaerobic conditions: a review. Anaerobe 15, 7–17.
Mellin, J., Tiensuu, T., Bécavin, C., Gouin, E., Johansson, J., Cossart, P., 2013. A riboswitch-regulated antisense RNA in *Listeria monocytogenes*. Proc. Natl. Acad. Sci. 110, 13132–13137.
Mengaud, J., Ohayon, H., Gounon, P., Mège, R.-M., Cossart, P., 1996. E-cadherin is the receptor for internalin, a surface protein required for entry of *L. monocytogenes* into epithelial cells. Cell 84, 923–932.
Moura, A., Lefrancq, N., Wirth, T., Leclercq, A., Borges, V., Gilpin, B., Dallman, T.J., Frey, J., Franz, E., Nielsen, E.M., Thomas, J., Pightling, A., Howden, B.P., Tarr, C.L., Gerner-Smidt, P., Cauchemez, S., Salje, H., Brisse, S., Lecuit, M., 2021. Emergence and global spread of *Listeria monocytogenes* main clinical clonal complex. Sci. Adv. 7, eabj9805.
Nadon, C.A., Bowen, B.M., Wiedmann, M., Boor, K.J., 2002. Sigma B contributes to PrfA-mediated virulence in *Listeria monocytogenes*. Infect. Immun. 70, 3948–3952.
Oliveira, M., Wijnands, L., Abadias, M., Aarts, H., Franz, E., 2011. Pathogenic potential of *Salmonella typhimurium* DT104 following sequential passage through soil, packaged fresh-cut lettuce and a model gastrointestinal tract. Int. J. Food Microbiol. 148, 149–155.
Osek, J., Wieczorek, K., 2022. *Listeria monocytogenes*-how this pathogen uses its virulence mechanisms to infect the hosts. Pathogens 11.
Pentecost, M., Otto, G., Theriot, J.A., Amieva, M.R., 2006. *Listeria monocytogenes* invades the epithelial junctions at sites of cell extrusion. PLoS Pathog. 2, e3.
Petit, E., LaTouf, W.G., Coppi, M.V., Warnick, T.A., Currie, D., Romashko, I., Deshpande, S., Haas, K., Alvelo-Maurosa, J.G., Wardman, C., 2013. Involvement of a bacterial microcompartment in the metabolism of fucose and rhamnose by *Clostridium phytofermentans*. PLoS One 8, e54337.
Portnoy, D.A., Auerbuch, V., Glomski, I.J., 2002. The cell biology of *Listeria monocytogenes* infection: the intersection of bacterial pathogenesis and cell-mediated immunity. J. Cell Biol. 158, 409–414.
Prentice, M.B., 2021. Bacterial microcompartments and their role in pathogenicity. Curr. Opin. Microbiol. 63, 19–28.
Prevention, C.f.D.C.a, 2003. Quantitative Assessment of the Relative Risk to Public Health From Foodborne *Listeria monocytogenes* Among Selected Categories of Ready-to-eat Foods. US Department of Agriculture–Food Safety and Inspection Service Washington, DC.
Radoshevich, L., Cossart, P., 2018. *Listeria monocytogenes*: towards a complete picture of its physiology and pathogenesis. Nat. Rev. Microbiol. 16, 32.
Raimann, E., Schmid, B., Stephan, R., Tasara, T., 2009. The alternative sigma factor σL of *L. monocytogenes* promotes growth under diverse environmental stresses. Foodborne Pathog. Dis. 6, 583–591.
Ravcheev, D.A., Moussu, L., Smajic, S., Thiele, I., 2019. Comparative genomic analysis reveals novel microcompartment-associated metabolic pathways in the human gut microbiome. Front. Genet. 10, 636.
Reniere, M.L., Whiteley, A.T., Portnoy, D.A., 2016. An in vivo selection identifies *Listeria monocytogenes* genes required to sense the intracellular environment and activate virulence factor expression. PLoS Pathog. 12, e1005741.
Salazar, J.K., Wu, Z., McMullen, P.D., Luo, Q., Freitag, N.E., Tortorello, M.L., Hu, S., Zhang, W., 2013. PrfA-like transcription factor gene lmo0753 contributes to L-rhamnose utilization in *Listeria monocytogenes* strains associated with human food-borne infections. Appl. Environ. Microbiol. 79, 5584–5592.
Schardt, J., Jones, G., Müller-Herbst, S., Schauer, K., D'Orazio, S.E., Fuchs, T.M., 2017. Comparison between *Listeria sensu stricto* and *Listeria sensu lato* strains identifies novel determinants involved in infection. Sci. Rep. 7, 17821.
Scortti, M., Monzó, H.J., Lacharme-Lora, L., Lewis, D.A., Vázquez-Boland, J.A., 2007. The PrfA virulence regulon. Microbes Infect. 9, 1196–1207.
Stewart, A.M., Stewart, K.L., Yeates, T.O., Bobik, T.A., 2021. Advances in the world of bacterial microcompartments. Trends Biochem. Sci. 46 (5), 406–416.
Sutter, M., Melnicki, M.R., Schulz, F., Woyke, T., Kerfeld, C.A., 2021. A catalog of the diversity and ubiquity of bacterial microcompartments. Nat. Commun. 12, 3809.
Szklarczyk, D., Gable, A.L., Lyon, D., Junge, A., Wyder, S., Huerta-Cepas, J., Simonovic, M., Doncheva, N.T., Morris, J.H., Bork, P., 2019. STRING v11: protein–protein association networks with increased coverage, supporting functional discovery in genome-wide experimental datasets. Nucleic Acids Res. 47, D607–D613.
Tang, S., Orsi, R.H., den Bakker, H.C., Wiedmann, M., Boor, K.J., Bergholz, T.M., 2015. Transcriptomic analysis of the adaptation of *Listeria monocytogenes* to growth on vacuum-packed cold smoked salmon. Appl. Environ. Microbiol. 81, 6812–6824.
Tasara, T., Stephan, R., 2006. Cold stress tolerance of *Listeria monocytogenes*: a review of molecular adaptive mechanisms and food safety implications. J. Food Prot. 69, 1473–1484.
Tattoli, I., Sorbara, M.T., Yang, C., Tooze, S.A., Philpott, D.J., Girardin, S.E., 2013. Listeria phospholipases subvert host autophagic defenses by stalling pre-autophagosomal structures. EMBO J. 32, 3066–3078.
Tsai, H.-N., Hodgson, D.A., 2003. Development of a synthetic minimal medium for *Listeria monocytogenes*. Appl. Environ. Microbiol. 69, 6943–6945.
Vizcaino, J.A., Csordas, A., del-Toro, N., Dianes, J.A., Griss, J., Lavidas, I., Mayer, G., Perez-Riverol, Y., Reisinger, F., Ternent, T., Xu, Q.W., Wang, R., Hermjakob, H., 2016. 2016 update of the PRIDE database and its related tools (vol 44, pg D447, 2016). Nucleic Acids Res. 44, 11033.
Vogt, J.A., Pencharz, P.B., Wolever, T.M., 2004. L-Rhamnose increases serum propionate in humans. Am. J. Clin. Nutr. 80, 89–94.
Yeates, T.O., Crowley, C.S., Tanaka, S., 2010. Bacterial microcompartment organelles: protein shell structure and evolution. Annu. Rev. Biophys. 39 (39), 185–205.
Zeng, Z., Smid, E.J., Boeren, S., Abee, T., 2019. Bacterial microcompartment-dependent 1, 2-propanediol utilization stimulates anaerobic growth of *Listeria monocytogenes* EGDe. Front. Microbiol. 10, 2660.
Zeng, Z., Boeren, S., Bhandula, V., Light, S.H., Smid, E.J., Notebaart, R.A., Abee, T., 2021a. Bacterial microcompartments coupled with extracellular electron transfer drive the anaerobic utilization of ethanolamine in *Listeria monocytogenes*. mSystems 6.
Zeng, Z., Li, S., Boeren, S., Smid, E.J., Notebaart, R.A., Abee, T., 2021b. Anaerobic growth of *Listeria monocytogenes* on rhamnose is stimulated by vitamin B(12) and bacterial microcompartment-dependent 1,2-propanediol utilization. mSphere 6, e0043421.
Zeng, Z., Wijnands, L.M., Boeren, S., Smid, E.J., Notebaart, R.A., Abee, T., 2021c. Impact of bacterial microcompartment-dependent ethanolamine and propanediol metabolism on *Listeria monocytogenes* interactions with Caco-2 cells. bioRxiv.
Zeng, Z., Dank, A., Smid, E.J., Notebaart, R.A., Abee, T., 2022. Bacterial microcompartments in food-related microbes. Curr. Opin. Food Sci. 43, 128–135.